JOURNAL OF
Materials
CHEMISTRY

The $MnPS_3$ layered phase as a substrate for aggregate formation: the example of triarylpyrylium cations

Thibaud Coradin,[a] Michèle Veber,[b] Anthony H. Francis[c] and René Clément*[a]

[a]*Laboratoire de Chimie Inorganique, URA 420, Université Paris-Sud, 91400 Orsay, France*
[b]*Laboratoire de Physique des Solides, URA 002, Université Paris-Sud, 91400 Orsay, France*
[c]*Department of Chemistry, The University of Michigan, Ann Arbor, MI 48109, USA*

Intercalation of triarylpyrylium salts into the $MnPS_3$ layered phase has been achieved. The formation of J-aggregates in the interlayer space is suggested on the basis of UV–VIS absorption and emission spectroscopy experiments. The extended dipole model approximation is used to derive structural information that appears consistent with the X-ray powder diffraction data. However, in contrast to previous results, none of the intercalates exhibit any second harmonic generation. Finally, the important influence of the host phase dielectric properties on aggregate formation is emphasized.

Since their discovery by Jelley[1] and Schiebe,[2] molecular aggregates have been the subject of numerous investigations not only from a theorical point of view in connection with the development of exciton theory,[3–6] but also in the applied fields of photographic imaging and optical devices.[7,8] In particular, it has been shown how aggregates formation can lead to highly non-linear optically (NLO) active materials.[9]

The main characteristic of molecular aggregation is the appearance of a red-shift (J-aggregates) or a blue-shift (H-aggregates) of the absorption band of the aggregates with respect to the monomer band.[10] Even though many examples of these molecular organizations have been reported[11–16] their mechanisms of formation and photophysical properties are not completely understood. In the case of cationic aggregates, formation depends on the balance between cation–anion, cation–solvent and cation–cation interactions.[17] Cation-exchangeable intercalation compounds are of interest because the interlamellar space can be viewed either as a counter anion or as a solvating medium.[18]

We have recently reported that intercalation of stilbazolium chromophores in the hexathiohypodiphosphate MPS_3 layered phases[19] (where M is a metal in the $+2$ oxidation state) could give rise to NLO active materials[20] and a model invoking the formation of J-aggregates in the interlamellar space of the host has been proposed.[21] A top view of the structural model of an MPS_3 slab is depicted in Fig. 1. In these systems, the formally $(2-)$ charged sulfur atoms delimiting the van der Waals space behave as a non-polar medium leading to weak host–guest interactions, thus favouring intermolecular interactions.

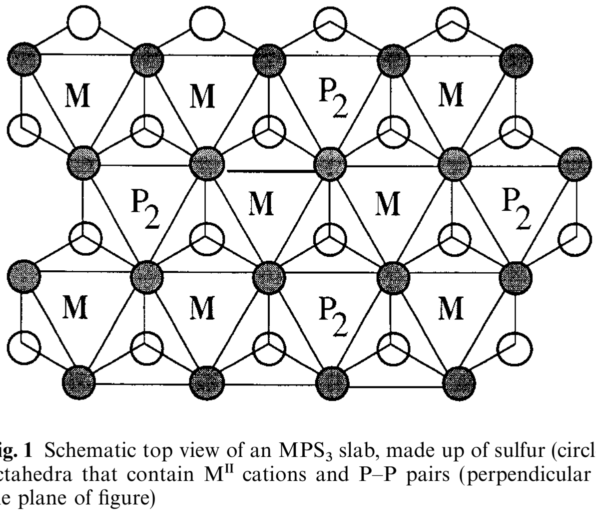

Fig. 1 Schematic top view of an MPS_3 slab, made up of sulfur (circles) octahedra that contain M^{II} cations and P–P pairs (perpendicular to the plane of figure)

To better understand this phenomenon, we have synthesized and intercalated a series of 2,4,6-triarylpyrylium salts in $MnPS_3$. The pyrylium cations have been reported to form aggregates in solution,[22,23] Langmuir–Blodgett films[24] and columnar liquid crystals.[25] The photophysical properties of these cationic aggregates have been extensively studied.[26–28] We have undertaken optical spectroscopic studies in order to determine the molecular organization of the cations in the interlamellar space of the $MnPS_3$ intercalates.

Experimental

Synthesis and characterization of the guest species

The three 2,4,6-triarylpyrylium salts **1a–c** (Scheme 1) studied in this work were obtained using already described procedures[22,23,29] by a two-step process involving the formation of the 2,6-diphenylpyrylium tetrafluoroborate followed by the addition of *N*,*N*-dimethylaniline **1a**, *N*,*N*-diethylaniline **1b** or *N*,*N*-didodecylaniline **1c**.

^1H NMR spectra of all species were recorded in $CDCl_3$ and compared with the values given in the literature. The study of the visible absorption spectra of 10^{-4}–10^{-5} M solutions showed an intense ($\varepsilon = 8 \times 10^4$ l mol^{-1} cm^{-1} in ethanol) band near 540 nm consistent with their deep purple colour, that has been attributed to a charge transfer from the dialkylaminophenyl group to the pyrylium ring.[30]

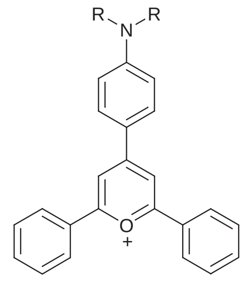

R = CH_3 (**1a**), C_2H_5 (**1b**), *n*-$C_{12}H_{25}$ (**1c**)

Scheme 1 Schematic representation of the 2,4,6-triarylpyrylium salts studied in this work

Synthesis and characterization of the intercalates

Pure $MnPS_3$ compound was synthesized by heating stoichiometric mixtures of the elements (purity 99.9%) in sealed evacuated quartz ampoules, following already described procedures.[31] Unless small or highly charged, cationic species do not easily enter MPS_3 host lattices: the interlamellar space usually needs to be pre-expanded using a solvated, highly mobile cation. For this purpose, $MnPS_3$ was first treated with a concentrated aqueous solution of tetramethylammonium chloride for 1 h, then washed and dried. 50 mg of the resulting $Mn_{1-x}PS_3(Me_4N)_{2x}(H_2O)_y$ pre-intercalate ($x \approx 0.85$) was then added to a 10 cm^3 ethanolic solution containing 100 mg of the triarylpyrylium salt and the mixture was heated overnight at 130 °C in a sealed evacuated Pyrex tube. The final highly coloured powder was washed several times with ethanol until the solution remained clear.

The X-ray powder diffraction patterns of the intercalates were recorded using a Siemens diffractometer. The powder was spread on a sample holder, and preferential orientation (due to the platelet shape of the grains) resulted in considerably enhanced intensity of the 00*l* reflections. IR spectra were obtained from KBr pressed disk samples using a Perkin Elmer 883 spectrometer.

Optical measurements

The UV–VIS absorption spectra were recorded between 800 and 350 nm. Samples were diluted from 0.1 to 1% in weight in dry KBr powder, repeatedly ground and pressed as pellets. Pure KBr was used as a reference for the double-beam mode of the Cary 5E spectrophotometer.

The emission spectra were recorded at room temperature and at 4.5 K. The room temperature studies were performed using a SPEX 1681 spectrofluorimeter on powders diluted in KBr pellets, using front-face excitation. The low temperature measurements were performed using a 5 W Coherent Argon ion laser, the samples being placed in a Janis 10DT cryostat cooled by liquid helium.

Low temperature photoluminescence was collected with an f/4 spherical lens and passed through a Corning 3–73 glass filter to eliminate scattered light from the excitation source. The luminescence was modulated with a mechanical chopper and dispersed with a 1/4 meter, f/4 aperture, Acton Research monochromator, and detected with a Hamamatsu 1695 photomultiplier tube. The photomultiplier tube has an S1 response which extends to 1250 nm and was cooled to −40 °C to reduce thermal noise. The signal from the photomultiplier was amplified by a PAR 124 lock-in amplifier.

The measurements of second harmonic generation (SHG) intensity were carried out using the Kurtz–Perry[32] powder technique, using a picosecond Nd–YAG pulsed (10 Hz) laser operating at 1.064 µm. Samples were unsized microcrystalline powders squeezed between two glass plates. After passing through the appropriate filters, the transmitted signal was detected by a photomultiplier and read on an ultrafast Tektronix 7834 oscilloscope. The SHG of a urea sample was used as the reference standard.

Results and Discussion

Intercalates characterization

Elemental analysis data are gathered in Table 1. The $MnPS_3$/**1a** and $MnPS_3$/**1b** compounds exhibit similar guest contents whereas the filling for $MnPS_3$/**1c** is smaller by nearly a half. This suggests different packing in the interlamellar space for **1c** as compared to **1a** and **1b** and is also consistent with the considerable space occupied by the two dodecyl aliphatic chains.

Successful intercalation of the three chromophores was also ascertained by powder X-ray diffraction. Disappearance of the 00*l* reflections of the pre-intercalate was taken as a criterion for complete insertion. The $MnPS_3$/**1a** and $MnPS_3$/**1b** intercalates displayed sharp 00*l* ($l = 1$–4) reflections allowing the calculation of basal spacings between 22 and 22.5 Å (6.5 Å for $MnPS_3$, Table 1). The van der Waals sizes of the **1a** and **1b** pyrylium molecules along the direction of the N···O axis and along the direction perpendicular to this axis are very close to each other, about 15 Å. As the thickness of the $MnPS_3$ slab is about 6.5 Å, the experimental values of the basal spacing of intercalates $MnPS_3$/**1a** and **1b** are consistent with an orientation of the guest molecules perpendicular to the layers. However, it is not possible to decide on the exact orientation of the N···O axis on the basis of van der Waals size only.

In sharp contrast, the $MnPS_3$/**1c** intercalate showed broader 00*l* ($l = 1$ to 2) peaks, indicating poorer crystallinity, and a basal spacing value of 10.7 Å, suggesting that the guest species lie with their molecular plane parallel to the layers. This orientation is consistent with the already observed organization of similar cations (methylviologen,[33] crystal violet[34]) in the MPS_3 van der Waals space. The difference observed in the orientation of **1a**, **1b** and **1c** may be attributed to the relative importance of guest–guest interactions and to the steric effect of the long aliphatic n-$C_{12}H_{25}$ chains that decreases the strength of such interactions. This effect could be enhanced by the fact that the pyrylium cations are not planar, the angle between the dialkylaminophenyl and the 2,4-diphenylpyrylium rings being theorically[35] and experimentally[23] estimated around 30 °C.

Attempts to prepare intercalates with a lower dye/$MnPS_3$ concentration failed; when the amount of reacting dye was too small, a diphasic solid consisting of fully loaded intercalate plus unreacted pre-intercalate was obtained.

The IR spectra of the intercalates showed numerous bands in the 2000–800 cm^{-1} wavenumber region that can be readily assigned to the chromophore species, plus an intense band consisting of two or three sharp components in the range 600–550 cm^{-1}. This feature is the usual signature of intercalation in these systems.[36] It has been assigned to the $\nu(P{-}S)$ asymmetric stretching band that occurs as a degenerate single band at 570 cm^{-1} in pristine MPS_3, the degeneracy being lifted as a consequence of the occurrence of intralamellar vacancies due to the departure of a fraction of the M^{2+} during intercalation. Finally, the absence of any strong band around 1100 cm^{-1} proves that BF_4^- counteranions are no longer present.

Optical measurements

The absorption spectra of the three intercalates are shown in Fig. 2, the spectrum of **1a** in ethanolic solution being repro-

Table 1 Analytical data and interlayer spacing of the intercalates

intercalate	analytical data (wt.%) C	H	N	O	P	S	Mn	spacing/Å
$Mn_{0.83}PS_3(\mathbf{1a})_{0.32}$	34.07	2.69	1.62	1.71	9.94	31.96	14.71	22
$Mn_{0.84}PS_3(\mathbf{1b})_{0.30}$	33.98	2.83	1.48	2.06	10.27	32.07	14.85	22.5
$Mn_{0.92}PS_3(\mathbf{1c})_{0.16}$	31.12	3.47	0.81	1.01	10.77	33.47	16.82	10.7

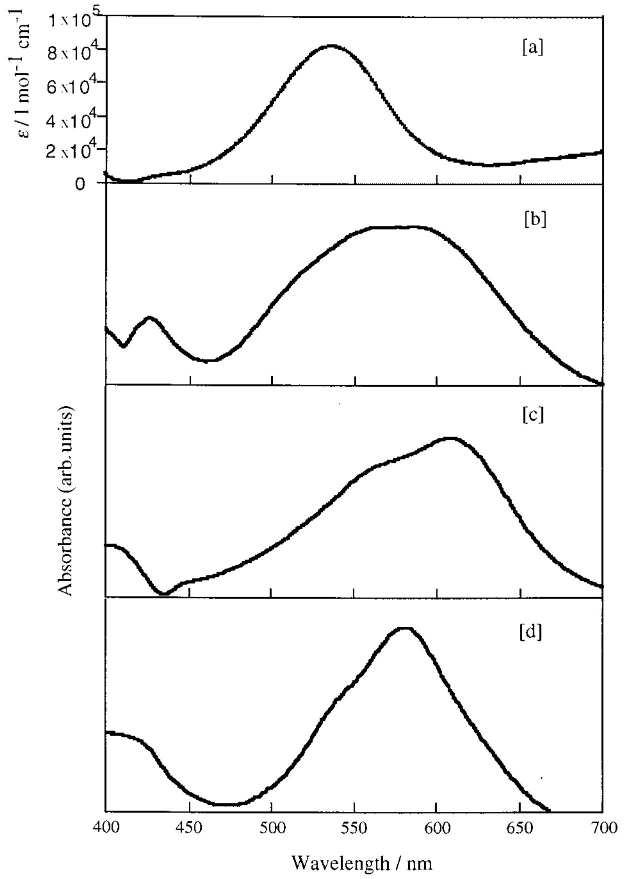

Fig. 2 UV–VIS absorption spectra of **1a** in ethanolic solution [a], $MnPS_3$/**1a** [b], $MnPS_3$/**1b** [c] and $MnPS_3$/**1c** [d] in KBr pellets

duced as a reference. The $MnPS_3$ host lattice does not absorb significantly above 400 nm, and therefore the bands shown are due to the inserted dyes only. A striking feature is the strong deformation of the band in the $MnPS_3$ intercalates and the appearance of a new maximum of absorption around 600 nm. An attempt to decompose the spectra of the intercalates revealed the possibility of analyzing them as the superposition of two bands: a first broad one (width *ca.* 3000 cm^{-1}) centered around 550 nm that corresponds to the maximum wavelength in solution and a sharper one (width *ca.* 1500 cm^{-1}) red-shifted by 40 to 60 nm (Table 2).The appearance of such bathochromically shifted bands can be related to the formation of dimers or J-aggregates.[37] However, the coexistence of two bands of various relative intensities seems to indicate that all the monomers do not form aggregates, some remaining isolated in the interlamellar space. Clearly, knowledge of the absorption spectrum of the intercalated monomer would be helpful to support the deconvolution results, but as pointed out above it was not possible to prepare a 'diluted' intercalate that would contain monomers only.

The suggested orientation for **1a** and **1b** would indicate strong intermolecular interactions between the aromatic rings of the chromophores, a situation already observed in the case of stilbazolium intercalation.[21] If the O···N axis of the guest species is perpendicular to the slabs, it is difficult to imagine how J-type aggregates can form. On the contrary, there is no steric hindrance if the O···N axis of the pyrylium species stands parallel to the layer: two adjacent pyrylium cations can stand parallel but shifted one with respect to the other, in such a way that the donating group of one molecule interacts with the accepting part of the neighbour. In the case of MnPS3/**1c**, formation of chains of interacting pyrylium species can also be envisaged readily, because the alkyl substituents can twist in order to allow intermolecular N···O approach. These postulated arrangements are depicted in Fig. 3. The occurrence of two different types of arangement is supported by the two very different basal spacings and also by the different shifts of the absorption band (larger for **1a**, **1b** than for **1c**).

Table 2 Absorption maximum wavelengths obtained from the decomposition of the intercalates UV–VIS band and the corresponding energy difference

	solution	$MnPS_3$ intercalate		
	λ/nm	λ_1/nm	λ_2/nm	(E_1-E_2)/cm^{-1}
1a	540	540	600	1850
1b	542	555	615	1750
1c	547	545	585	1250

The frequency shift associated with the aggregation process arises from the interaction between the transition dipoles of the ordered chromophores. In the framework of the extended-dipole model approximation proposed by Kuhn and coworkers,[38,39] molecules are represented by dipoles of charge ε and length l defined by

$$M=\varepsilon l \tag{1}$$

In this model, the electric dipole moment M is used as an approximation of the transition moment of the monomer. Note that, in the case of the triarylpyrylium chromophores studied in this work, the charge transfer associated with the transition can be considered as one-dimensional so that the transition dipole direction corresponds roughly to the nitrogen–oxygen molecular axis.

The transition energy $\Delta E'$ for the aggregate can then be expressed as

$$\Delta E'=\Delta E\pm 2J_{12} \tag{2}$$

where ΔE is the transition energy of the monomer and J_{12} is the interaction energy between adjacent molecules that depends on the relative orientation of the chromophores (Scheme 2); the sign ± correspond to the in-phase and out-of-phase combinations of the monomer transition moments, respectively.

Application of this model to our systems led to two main results. First, the appearance of a single aggregate band

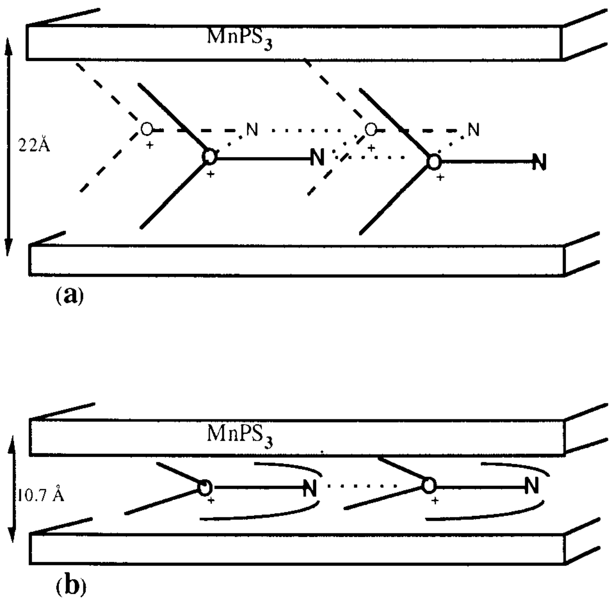

Fig. 3 Tentative representation of the proposed aggregation processes in (a) $MnPS_3$/**1a,b**; (b) $MnPS_3$/**1c**

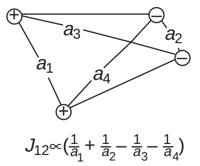

Scheme 2 Schematic representation of two interacting chromophores in the extended-dipole model and the corresponding J_{12} interaction energy

indicates that one of the two combinations of monomer transition moments is equal to zero: this is consistent with the case where the interacting chromophores have their molecular planes parallel. Then, since the aggregate band lies at lower energy than the monomer energy transition, the second term of eqn. (2) must have a negative value. This is true if J_{12} is positive and the out-of-phase combination of transition moments non equal to zero or if J_{12} is negative and the in-phase combination of transition moments non-equal to zero. Taking into account the fact that molecules can adopt either a 'head-to-tail' or an 'aligned' orientation, the four limiting configurations shown in Scheme 3 were considered.

In configuration 1, J_{12} is positive but the out-of-phase combination is equal to zero. On the contrary, in configuration 2, J_{12} is negative but the in-phase combination is also equal to zero. So, only configurations 3 and 4 seem to correspond to the observed absorption spectra. Two elements are in favour of these structures: first, it would explain that the aggregates can be formed if the molecules are standing 'edge-on' or parallel to the $MnPS_3$ layers. Then it would explain the decrease in the $|J_{12}|$ value as the aliphatic chain on the amino group is lengthened. Finally, from an electrostatic point of view, it can be assumed that formally donor dialkylamino group interacts preferentially with the positive acceptor pyrylium group, thus favouring the configuration 3.

Emission spectra were recorded at room temperature by excitation at the two absorption maximum wavelengths but no significant luminescence was detected. However, at 4.5 K, excitation at 480 nm led to emission bands in the 600–750 nm range (Fig. 4). In the case of $MnPS_3$/**1a**, a broad band centered around 650 nm with a shoulder around 730 nm was observed. In contrast, $MnPS_3$/**1b** showed a single sharp luminescence band centered at 730 nm. Finally, $MnPS_3$/**1c** exhibited a sharp emission band at 660 nm and a shoulder around 730 nm. The presence of luminescence bands around 650 and 730 nm has already been reported for **1c** in solution,[23] the first band corresponding to the isolated cation and the second band attributed to aggregates. Interpretation of these luminescence spectra is not straightforward, particularly their relation to the absorption spectra. The absorption and emission data appear reasonably consistent for $MnPS_3$/**1b**: main band of the absorption spectrum (615 nm) attributed to aggregates and sharp luminescence at 730 nm also attributable to aggregates. Interpretation is less clear for $MnPS_3$/**1a**: most of the luminescence intensity is centered around 650 nm and indicates predominance of monomers; the absorption spectrum has a strong component at 550 nm also attributable to monomers. The absorption band at 615 nm is smaller than that for $MnPS_3$/**1b** and may correspond to the small emission shoulder at 730 nm. However the important width of the absorption band might also be partly due to solid state broadening (as previously observed in $ZnPS_3$–stilbazolium non-aggregated intercalates[21]) and then the aggregate/monomer ratio might be small, as suggested by the emission band that only shows a weak shoulder at 730 nm. Clearly the lack of spectral data for inserted pure monomers is a severe handicap.

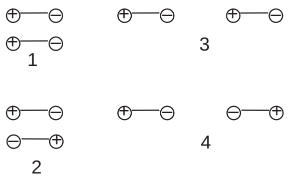

Scheme 3 Schematic representation of the four limiting configurations for two parallel interacting dipoles

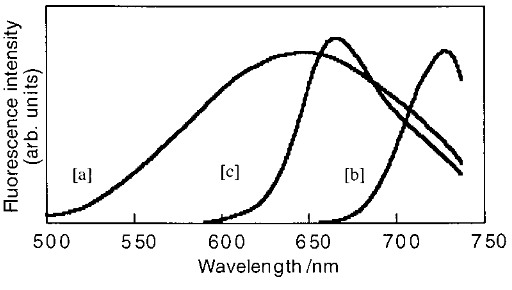

Fig. 4 Emission spectra of $MnPS_3$/**1a** [a], $MnPS_3$/**1b** [b] and $MnPS_3$/**1c** [c] recorded at 4.5 K at $\lambda_{exc} = 480$ nm

The data obtained for $MnPS_3$/**1c** also raise difficult questions: the red shift of the main absorption band (with respect to solution monomer) is smaller than that for the other intercalates, only 40 nm: this may be due to the occurrence of a different type of aggregate that would involve weaker guest–guest interactions, as suggested on Fig. 3(b). However the shift of the absorption band may also arise from the interaction of **1c** monomers with the host lattice. Actually the orientation of **1c** species (parallel to the slabs) can obviously favor host–guest interactions. The emission band given by $MnPS_3$/**1c** is very similar to that of the monomer, and hence this possibility cannot be ruled out.

The luminescence spectra of $MnPS_3$/**1a**,**b**,**c** therefore suggest very different organizations of the chromophores for the three intercalates together with important variations in the aggregate-to-monomer ratio.

Finally, none of the intercalates exhibited any significant SHG efficiencies indicating an average centrosymmetrical organization. This can happen either if the chromophore packing is locally centrosymmetric or if the dimension of non-centrosymmetric aggregates is less than the coherence length. This contrasts with our previous work on stilbazolium chromophores intercalation,[21] underlying the non-trivial relationship between aggregate formation and SHG properties.

A final remark must be made concerning the influence of the MPS_3 host lattice on aggregate formation. It has been reported that **1c** exists as a monomer in methanol and forms dimers in chloroform and toluene,[23] thus underlining the importance of the polarity of the solvating medium. Solvatochromic studies[40] were performed using a series of highly polarizable stilbazolium chromophores in order to compare the polarity of the MPS_3 van der Waals space with usual organic solvents. The observed bathochromic shift of the stilbazolium charge transfer bands following on intercalation corresponds to a dielectric constant ε_r value in the range 5–7 consistent with a weakly polar media in which the **1c** dimerization process occurs ($\varepsilon_r[CHCl_3] = 4.81$). Thus, since the intercalation reaction is performed in ethanol where the triarylpyrylium cations stand as monomers, it can be assumed that the aggregation process takes place once the chromophores are inserted or in the vicinity of the MPS_3 surface. In favour of this last hypothesis are the rigid nature of the MPS_3 layers making difficult any molecular reorganizations of the inserted species and the slow kinetics of the intercalation process consistent with a strong steric effect due to bulky dimers.

In conclusion, this paper reports a new example of aggregation in the MPS_3 layered phases. Since this phenomenon is currently of great interest in optics, these materials appear to be good candidates for further theoretical and photophysical work. Some MPS_3 intercalates are currently being studied by XPS spectroscopy in order to obtain more information on the effects of intercalation and aggregation on the electronic properties of the chromophores. Moreover, because of the important energy delocalization usually associated with aggregation, such systems might exhibit large third order NLO efficiencies.

The authors thank Dr. K. Nakatani (Cachan) for the NLO measurements. Support by European COST Action D4/0001/95 is kindly acknowledged.

References

1 E. E. Jelley, *Nature (London)*, 1936, **138**, 1009.
2 G. Scheibe, *Angew. Chem.*, 1939, **42**, 631.
3 A. S. Davydov, *J. Exptl. Theoret. Phys.*, 1948, **18**, 210.
4 E. G. McRae and M. Kasha, *J. Chem. Phys.*, 1958, **28**, 721.
5 M. Kasha, H. R. Rawls and M. A. El-Bayoumi, *Pure Appl. Chem.*, 1965, **11**, 371.
6 H. Kuhn and W. Huber, *Helv.*, 1959, **42**, 363.
7 M. T. Spitler, *J. Chem. Educ.*, 1983, **60**, 330.
8 P. M. Borsenberger, A. Chowdry, D. C. Hoesterey and W. Mey, *J. Appl. Phys.*, 1978, **49**, 5555.
9 S. Yitzchaik, S. Di Bella, P. M. Lundquist, G. K. Wong and T. J. Marks, *J. Am. Chem. Soc.*, 1997, **119**, 2995.
10 E. Rabinowitch and L. F. Epstein, *J. Am. Chem. Soc.*, 1941, **63**, 69.
11 V. Mizrahi, G. I. Stegemen and W. Knoll, *Phys. Rev. A*, 1989, **39**, 3555.
12 C. E. Evans and P. W. Bohn, *J. Am. Chem. Soc.*, 1993, **115**, 3306.
13 B. Lebeau, N. Herlet, J. Livage and C. Sanchez, *Chem. Phys.*, 1993, **206**, 15.
14 W. F. Mooney, P. E. Brown, J. C. Russel, S. B. Costa, L. G. Pedersen and D. G. Whitten, *J. Am. Chem. Soc.*, 1984, **106**, 5659.
15 V. Sundström and T. Gillbro, *J. Chem. Phys.*, 1985, **83**, 2733.
16 K. Fidder, J. Knoester and D. A. Wiersma, *J. Chem. Phys.*, 1993, **98**, 15.
17 M. Schubert and A. Levine, *J. Am. Chem. Soc.*, 1955, **77**, 4197.
18 G. Calzaferri and N. Gfeller, *J. Phys. Chem.*, 1988, **20**, 3007.
19 R. Brec, *Solid State Ionics*, 1986, **22**, 3.
20 P. G. Lacroix, R. Clément, K. Nakatani, J. Zyss and I. Ledoux, *Science*, 1994, **263**, 658.
21 T. Coradin, R. Clément, P. G. Lacroix and K. Nakatani, *Chem. Mater.*, 1996, **8**, 2153.
22 D. Markovitsi, C. Jallabert, H. Strzelecka and M. Veber, *J. Chem. Soc., Faraday Trans.*, 1990, **86**, 2819.
23 I. Lampre, D. Markovitsi, N. Birlirakis and M. Veber, *Chem. Phys.*, 1996, **202**, 107.
24 C. Ecoffet, D. Markovitsi, M. Vandyver, A. Barraud, M. Veber, C. Jallabert, H. Strzelecka and P. A. Albouy, *Thin Solid Films*, 1992, **211**, 586.
25 C. Ecoffet, D. Markovitsi, C. Jallabert, H. Strzelecka and M. Veber, *Thin Solid Films*, 1994, **242**, 83.
26 A.T. Balaban, A. Dinculescu, G. N. Dorofeenko, G. W. Fisher, A. V. Koblik, V. V. Mezheritskii and W. Shroth, *Pyrilium Salts, Synthesis, Reactions and Physical Properties*, Academic Press, New York, 1982
27 C. Ecoffet, D. Markovitsi, C. Jallabert, H. Strzelecka and M. Veber, *J. Chem. Soc., Faraday Trans.*, 1992, **88**, 3007.
28 C. Ecoffet, D. Markovitsi, P. Millié, C. Jallabert, H. Strzelecka and M. Veber, *J. Chem. Soc., Faraday Trans.*, 1993, **89**, 457.
29 G. A. Reynolds, C. H. Chen and J. A. Van Allan, *J. Org. Chem.*, 1979, **44**, 4456.
30 J. R. Wilt, G. A. Reynolds and J. A. Van Allan, *Tetrahedron,* 1973, **29**, 795.
31 W. Klingen, R. Ott and H. Hahn, *Z. Anorg. Allg. Chem.*, 1973, **396**, 271.
32 S. K. Kurtz and T. T. Perry, *J. Appl. Phys.*, 1968, **39**, 3798.
33 A. Léaustic, J. P. Audière, D. Cointereau, R. Clément, L. Lomas, F. Varret and H. Constant-Machado, *Chem. Mater.*, 1996, **8**, 1954.
34 E. Manova and R. Clément, unpublished work.
35 D. Markovitsi, H. Sigal, C. Ecoffet, P. Millié, F. Charra, C. Fiorini, J. M. Nunzi, H. Strzelecka, M. Veber and C. Jallabert, *Chem. Phys.*, 1994, **182**, 69.
36 C. Sourisseau, J. P. Forgerit and Y. Mathey, *J. Solid State Chem.*, 1983, **49**, 134.
37 D. Möbius, *Adv. Mater.*, 1995, **7**, 437.
38 V. Czikkely, G. Dreizler, H. D. Försterling, H. Kuhn, J. Sondermann, P. Tillmann and J. Wiegand, *Z. Naturforsch.*, 1969, **24**, 1821.
39 V. Czikkely, H. D. Försterling and H. Kuhn, *Chem. Phys. Lett.*, 1970, **6**, 207.
40 T. Coradin, PhD Thesis, University of Paris-Sud, France, 1997

Paper 8/01068D; *Received* 5*th February*, 1998